European Journal of Mechanical Engineering Research, 12(2),61-78, 2025

Print ISSN: 2055-6551(Print)

Online ISSN: 2055-656X(Online)

Website: https://www.eajournals.org/

Publication of the European Centre for Research Training and Development-UK

Analysis of Steady and Transient Free Convection of Nanofluids in a Vertical Channel: Combined Analytical and Numerical Approaches

M. N. Sarki[1] and A. Buhari[*, 2]

[1]Abdullahi Fodio University of Science and Technology Aliero, Kebbi State, Nigeria.

[2]Federal University Birnin Kebbi, Kebbi State, Nigeria.

doi: https://doi.org/10.37745/ejmer.2014/vol12n26178 Published December 30, 2025

Citation: Sarki M.N. and A. Buhari (2025) Analysis of Steady and Transient Free Convection of Nanofluids in a Vertical Channel: Combined Analytical and Numerical Approaches, *European Journal of Mechanical Engineering Research*, 12(2),61-78

Abstract: *This study presents closed-form analytical and numerical solutions for both steady and transient free convection flow of a nanofluid in a vertical channel. The mathematical model is based on the Buongiorno model, incorporating the effects of Brownian motion and thermophoresis. Exact solutions for the steady-state velocity, temperature, and nanoparticle concentration profiles are derived using the method of separation of variables. For the transient regime, a semi-analytical solution is obtained using the Laplace transform technique after a linearization of the governing equations. Numerical validation is performed using an Implicit Finite Difference Method (IFDM), with stability assured by Von Neumann analysis. The influence of key dimensionless parameters such as Grashof number (*Gr*), buoyancy ratio (*Nr*), Brownian motion (*Nb*), and thermophoresis (*Nt*) are investigated comprehensively. Results indicate that increasing* Gr *from 1 to 10 enhances the maximum velocity by 637%, while increasing* Nr *from 0.5 to 2.0 dampens the flow intensity by 23%. Transient analysis reveals significant overshoots in Nusselt (*Nu*) and Sherwood (*Sh*) numbers, reaching up to 40% and 28% above their steady-state values, respectively, highlighting enhanced heat and mass transfer during the initial stages. The analytical solutions provide excellent benchmarks, showing perfect agreement with numerical results and deviations of less than 1% from established literature.*

Keywords: analytical solution, free convection, heat transfer enhancement, laplace transform, nanofluid, transient flow, vertical channel,

INTRODUCTION

The thermal performance of conventional heat transfer fluids like water and ethylene glycol is inherently limited by their low thermal conductivity. The advent of nanofluids "engineered colloidal suspensions of nanoparticles (1–100 nm) in base fluids" has opened new frontiers in thermal management, offering enhancements in thermal conductivity of up to 40% [1]. The pioneering work of Choi [2] first introduced the concept of nanofluids. Subsequent model by Buongiorno [3],

which identified Brownian diffusion and thermophoresis as the primary slip mechanisms, laid the foundation for understanding nanofluid dynamics.

Free convection in vertical channels is a fundamental configuration with widespread applications in electronics cooling, solar energy systems, and building ventilation. While numerous studies have investigated steady-state convection [4, 5], the analysis of transient behavior remains relatively scarce, despite its critical importance for systems subject to startup, shutdown, or fluctuating thermal loads. Most existing studies rely heavily on numerical simulations [6], with a notable lack of closed-form analytical solutions, particularly for the transient regime. Such analytical solutions are indispensable for validating numerical codes and gaining deeper physical insights into the coupled dynamics of heat and mass transfer.

Grosan and Pop [7] provided analytical solutions for mixed convection in a vertical channel, but their focus was on steady-state conditions. Studies addressing transient nanofluid flow often employ full numerical approaches [8], leaving a gap for verifiable analytical frameworks. The present study aims to bridge this gap by deriving exact analytical solutions for both steady and transient free convection in a vertical channel.

The key objectives of this work are:

i. To formulate and solve the steady-state governing equations analytically using separation of variables.
ii. To develop a semi-analytical solution for the transient governing equations using the Laplace transform method.
iii. To validate the analytical solutions with a numerical scheme based on the Implicit Finite Difference Method (IFDM).
iv. To conduct a comprehensive parametric study on the influence of Gr, Nr, Nb, and Nt on the flow, thermal, and concentration fields, as well as on the heat and mass transfer rates.

Mathematical Formulation

Physical Model and Governing Equations

Consider a laminar, incompressible flow of a nanofluid between two infinite vertical parallel plates separated by a distance L. The coordinate system is chosen such that the x-axis is aligned vertically against gravity, and the y-axis is perpendicular to the channel walls, located at $y = 0$ and $y = L$. The temperatures and nanoparticle concentrations at the walls are maintained at $(\mathrm{T}_1, \mathrm{C}_1)$ and $(\mathrm{T}_2, \mathrm{C}_2)$, respectively, with $\mathrm{T}_2 > \mathrm{T}_1$. The flow is driven solely by buoyancy forces (free convection).

European Journal of Mechanical Engineering Research, 12(2),61-78, 2025

Print ISSN: 2055-6551(Print)

Online ISSN: 2055-656X(Online)

Website: https://www.eajournals.org/

Publication of the European Centre for Research Training and Development-UK

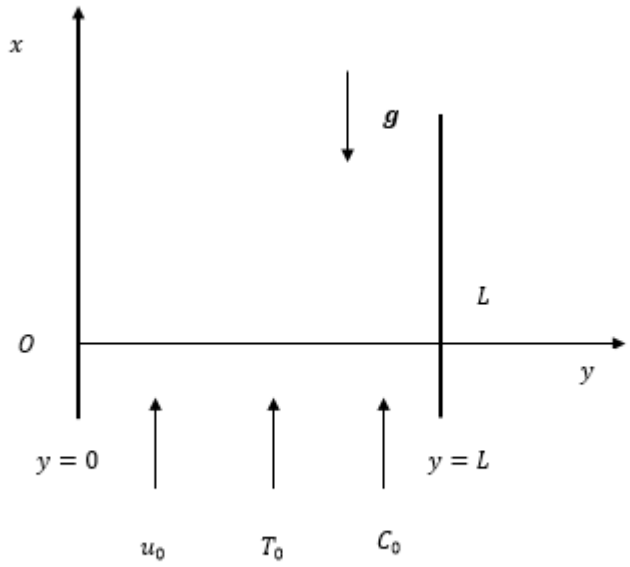

Fig. 1: Physical Configuration of the Flow

Under the Oberbeck-Boussinesq approximation and assuming a dilute nanoparticle concentration, the dimensional governing equations for mass, momentum, energy, and nanoparticle concentration are:

$$\nabla \cdot \boldsymbol{v} = 0 \tag{1}$$

$$\rho_f \left(\frac{\partial v}{\partial t} + \boldsymbol{v} \cdot \nabla \boldsymbol{v}\right) = -\nabla p + \mu \nabla^2 \boldsymbol{v} + \left[(\rho_p - \rho_{f0})(C - C_0) - (1 - C_0)\rho_{f0}\beta(T - T_0)\right]\boldsymbol{g} \tag{2}$$

$$(\rho c)_f \left(\frac{\partial T}{\partial t} + \boldsymbol{v} \cdot \nabla \boldsymbol{T}\right) = k\nabla^2 \boldsymbol{T} + (\rho c)_p \left[D_B \nabla C \cdot \nabla \boldsymbol{T} + \frac{D_T}{T_0} \nabla \boldsymbol{T} \cdot \nabla \boldsymbol{T}\right] \tag{3}$$

$$\frac{\partial C}{\partial t} + \boldsymbol{v} \cdot \nabla C = D_B \nabla^2 C + \frac{D_T}{T_0} \nabla^2 \boldsymbol{T} \tag{4}$$

To derive the simplified governing equations for the present problem, we introduce the following key assumptions:

1. Fully Developed Flow: The flow is hydrodynamically and thermally fully developed. This implies that the velocity and temperature profiles do not change in the primary flow direction (x-direction). Hence, the derivatives with respect to x*x* vanish

$$\frac{\partial u}{\partial x} = 0, \ \frac{\partial T}{\partial x} = 0, \ \frac{\partial C}{\partial x} = 0 \tag{5}$$

Consequently, the velocity field reduces to $v = (u(y), 0)$.

2. Parallel Plates and Constant Pressure Gradient: For free convection between infinite vertical parallel plates driven solely by buoyancy, the pressure gradient in the y-direction is zero ($\frac{\partial p}{\partial y} =$

0), and the axial pressure gradient $\frac{\partial p}{\partial x}$ is constant. For the case of no imposed pressure gradient, this constant is zero.

3. Linearization of the Buoyancy Term: The Boussinesq approximation is applied, and the buoyancy term in the momentum equation is linearized. We define the reference state (T_0, C_0) as the average of the boundary conditions ($T_0 = \frac{T_1+T_2}{2}$ and $C_0 = \frac{C_1+C_2}{2}$). The density variation is approximated as

$$\rho - \rho_{f0} \approx -\rho_{f0}\beta(T - T_0) + (\rho_p - \rho_{f0})(C - C_0) \quad (6)$$

where the term $C_0\beta(T - T_0)$ is neglected for dilute nanoparticle concentrations.

Applying these assumptions to the general governing equations (1)-(4), the continuity equation (1) is identically satisfied. The x-component of the momentum equation (2) simplifies significantly. The transient and convective terms ($\frac{\partial u}{\partial t}$ and $\boldsymbol{v} \cdot \nabla \boldsymbol{v}$) vanish due to the steady-state and fully developed assumptions. The pressure gradient $\frac{\partial p}{\partial x}$ is zero for pure free convection. Thus, the momentum equation reduces to a balance between viscous forces and buoyancy forces. And under the fully developed flow assumption, the energy equation (3) and concentration equation (4) lose their transient and axial advection terms. The resulting equations, which now consider diffusion and the cross-coupling terms of Brownian motion and thermophoresis in the y-direction, are given by Equations (8) and (9), respectively.

$$\mu\frac{d^2u}{dy^2} + \left[(1 - C_0)\rho_{f0}\beta(T - T_0) - \left(\rho_f - \rho_{f0}\right)(C - C_0)\right]g = 0 \quad (7)$$

$$k\frac{d^2T}{dy^2} + (\rho c)_p\left[D_B\frac{dC}{dy}\frac{dT}{dy} + \left(\frac{D_T}{T_0}\right)\left(\frac{dT}{dy}\right)^2\right] = 0 \quad (8)$$

$$D_B\frac{d^2C}{dy^2} + \left(\frac{D_T}{T_0}\right)\frac{d^2T}{dy^2} = 0 \quad (9)$$

and are subjected to the boundary conditions

$$\left.\begin{array}{ll} u = 0,\ T = T_1,\ C = C_1 & \text{at } y = 0 \\ u = 0,\ T = T_2,\ C = C_2 & \text{at } y = L \end{array}\right\} \quad (10)$$

introducing the following dimensionless variables

$$\left.\begin{array}{c} Y = \frac{y}{L},\ U(Y) = \frac{u(y)}{u_0},\ P(Y) = \frac{p(y)}{\rho u_0^2} \\ \theta(Y) = \frac{(T-T_0)}{(T_2-T_0)},\ \emptyset(Y) = \frac{(C-C_0)}{(C_2-C_0)} \end{array}\right\} \quad (11)$$

Steady-State Dimensionless Equations

For fully developed steady-state flow, the governing equations reduce to the following dimensionless forms, introducing the dimensionless variables in Eq. (11):

$$\frac{d^2U}{dY^2} + Gr\,\theta(Y) - Nr\,\phi(Y) = 0 \quad (12)$$

$$\frac{d^2\theta}{dY^2} + Pr\left[Nb\frac{d\phi}{dY}\frac{d\theta}{dY} + Nt\left(\frac{d\theta}{dY}\right)^2\right] = 0 \quad (13)$$

$$\frac{d^2\phi}{dY^2} + \frac{Nt}{Nb}\frac{d^2\theta}{dY^2} = 0 \quad (14)$$

The corresponding boundary conditions are:

$$\left.\begin{array}{c} U(0)=0,\ \theta(0)=-1,\ \phi(0)=-1 \\ U(1)=0,\ \theta(1)=1,\ \phi(1)=1 \end{array}\right\} \quad (15)$$

The dimensionless parameters are defined as:

$$\left.\begin{array}{c} Gr=\frac{(1-C_0)g\beta(T_2-T_0)L^3}{\nu^2},\ Nr=\frac{(\rho_p-\rho_f)g(C_2-C_0)L^2}{\mu u_0},\ Pr=\frac{\nu}{\alpha} \\ Nb=\frac{(\rho c)_p D_B(C_2-C_0)}{(\rho c)_f \alpha},\ Nt=\frac{(\rho c)_p D_T(T_2-T_0)}{(\rho c)_f \alpha T_0} \end{array}\right\} \quad (16)$$

Transient Dimensionless Equations

The dimensionless transient governing equations are:

$$\frac{\partial U}{\partial \tau}=\frac{\partial^2 U}{\partial Y^2}+Gr\,\theta(Y,\tau)+Nr\,\phi(Y,\tau) \quad (17)$$

$$\frac{\partial \theta}{\partial \tau}=\frac{1}{Pr}\frac{\partial^2 \theta}{\partial Y^2}+\frac{Nb}{Pr}\frac{\partial \phi}{\partial Y}\frac{\partial \theta}{\partial Y}+\frac{Nt}{Pr}\left(\frac{\partial \theta}{\partial Y}\right)^2 \quad (18)$$

$$\frac{\partial \phi}{\partial \tau}=\frac{1}{Le}\frac{\partial^2 \phi}{\partial Y^2}+\frac{1}{Le}\frac{Nt}{Nb}\frac{\partial^2 \theta}{\partial Y^2} \quad (19)$$

The initial and boundary conditions are:

$$\left.\begin{array}{c} U(Y,0)=0,\theta(Y,0)=\theta_0(Y),\phi(Y,0)=\phi_0(Y) \\ U(0,\tau)=0,\theta(0,\tau)=-1,\phi(0,\tau)=-1 \\ U(1,\tau)=0,\theta(1,\tau)=1,\phi(1,\tau)=1 \end{array}\right\} \quad (20)$$

SOLUTION METHODOLOGY

Steady-State Analytical Solution

The coupled system of Equations (12)-(14) is solved analytically. Integrating Eq. (14) twice yields a linear relationship between concentration and temperature:

$$\phi(Y)=-\frac{Nt}{Nb}\theta(Y)+AY+B \quad (21)$$

where constants A and B are determined from boundary conditions.

Substituting Eq. (21) into Eq. (13) simplifies the energy equation to a linear second-order ODE:

$$\frac{d^2\theta}{dY^2}+Pr\,Nb\,A\frac{d\theta}{dY}=0 \quad (22)$$

Solving Eq. (22) and applying boundary conditions gives the temperature profile:

$$\theta(Y)=C_3+C_4e^{-C_2PrY} \quad (23)$$

where $C_2 = Nb\,A$, and C_3, C_4 are integration constants.

The concentration profile is then obtained from Eq. (21)

$$\phi(Y)=-\frac{Nt}{Nb}(C_3+C_4e^{-C_2PrY})+C_1Y-\frac{C_1}{2} \quad (24)$$

and the velocity profile is found by integrating the momentum equation (12):

$$U(Y)=\frac{C_5}{C_2^2Pr^2}+\left[\frac{C_7}{2}+\frac{C_6}{6}-\frac{C_5}{C_2^2Pr^2}+\frac{C_5}{C_2^2Pr^2}e^{-C_2Pr}\right]Y-\frac{C_7}{2}Y^2-\frac{C_6}{6}Y^3-\frac{C_5}{C_2^2Pr^2}e^{-C_2PrY} \quad (25)$$

The constants C_1 to C_7 are defined in terms of Gr, Nr, Nb, Nt, and Pr as

$$\left.\begin{aligned} C_1 = 2\left(1+\frac{Nt}{Nb}\right),\ C_2 = NbC_1,\ C_3 = \frac{(e^{C_2Pr}+1)}{(e^{C_2Pr}-1)} \\ C_4 = -\frac{2e^{C_2Pr}}{(e^{C_2Pr}-1)},\ C_5 = C_4\left(Gr + Nr\frac{Nt}{Nb}\right),\ C_6 = -NrC_1, \\ C_7 = C_3\left(Gr + Nr\frac{Nt}{Nb}\right) + \frac{NrC_1}{2} \end{aligned}\right\} \quad (26)$$

The Nusselt and Sherwood numbers at the left wall (Y=0) are:

$$\left.\begin{aligned} Nu = -\theta'(0) = C_4C_2Pr \\ Sh = -\phi'(0) = -\left(\frac{Nt}{Nb}C_4C_2Pr + C_1\right) \end{aligned}\right\} \quad (27)$$

Transient Semi-Analytical Solution

The nonlinear transient system (Eqs. 17-19) is linearized to make the Laplace transform technique tractable. The nonlinear terms in the energy equation are approximated around the initial steady-state profiles, $\theta_0(Y)$ and $\phi_0(Y)$. The concentration equation is postulated to maintain the linear form of Eq. (21) during the transient.

Applying the Laplace transform, the system is solved in the s-domain. The inverse transform yields the transient solutions:

$$\theta(Y,\tau) = \theta_0 + \sum_{n=1}^{\infty} A_n \sin(n\pi Y)\, e^{-\lambda_n \tau} \quad (28)$$

where $\lambda_n = \frac{n^2\pi^2}{Pr} + \frac{Nbn\pi}{Pr}\frac{d\phi_0}{dY}$

$$\phi(Y,\tau) = \phi_0 - \frac{Nt}{Nb}\sum_{n=1}^{\infty} A_n \sin(n\pi Y)\, e^{-\lambda_n \tau} \quad (29)$$

$$U(Y,\tau) = U_0 + \sum_{n=1}^{\infty}\left[B_n \sin(n\pi Y)\, e^{-n^2\pi^2\tau} + C_n \sin(n\pi Y)\left(1 - e^{-\lambda_n\tau}\right)\right] \quad (30)$$

Coefficients A_n, B_n, C_n are determined from initial conditions and orthogonality.

Numerical Solution

An Implicit Finite Difference Method (IFDM) is employed to solve the full, nonlinear governing equations, providing a benchmark for the analytical solutions. The discretized equations form a tridiagonal system solved using the Thomas algorithm. A grid independence study established an optimal grid size of $N = 161$ ($\Delta Y = 0.0063$). Von Neumann analysis confirmed the unconditional stability of the implicit scheme.

RESULTS AND DISCUSSION

Validation and Grid Independence

The numerical model was rigorously validated. A grid independence study (Table 1) showed that a grid of $N = 161$ nodes provides a solution independent of mesh size. Benchmarking against Kuznetsov & Nield [4] for a vertical plate and Sarki & Buhari [5] for a vertical channel showed excellent agreement, with maximum deviations of 0.78% and 0.96%, respectively as shown in

table (2 and 3). The transient analytical and numerical solutions showed perfect convergence (Table 4), with errors on the order of 10^{-6}.

Table 1: Grid Independence Study ($Gr = 5, Nr = 0.5, Nb = 0.1, Nt = 0.1, Pr = 6.2$)

Grid	N	$\boldsymbol{\Delta Y}$	$\boldsymbol{U(0.5)}$	Rel. Error (%)	Time (s)
5	81	0.0125	0.252194	15.48	0.804
8	161	0.0063	0.218391	0.00	1.330

Table 2: Comparison with Kuznetsov & Nield (2010) Pure Free Convection Benchmark

$\boldsymbol{Y}$ Position	Present Study $\boldsymbol{U(Y)}$	Kuznetsov & Nield $\boldsymbol{U(Y)}$	Deviation (%)
$\mathbf{0.0}$	0.0000	0.0000	0.00
$\mathbf{0.1}$	0.0894	0.0901	0.78
$\mathbf{0.3}$	0.2047	0.2058	0.53
$\mathbf{0.5}$	0.2452	0.2460	0.33
$\mathbf{0.7}$	0.2186	0.2193	0.32
$\mathbf{0.9}$	0.1128	0.1134	0.53
$\mathbf{1.0}$	0.0000	0.0000	0.00

Table 3: Comparison with Sarki & Buhari (2025) Analytical Solution for Free Convection

Parameter	Present Study (Numerical)	Sarki & Buhari (2025) (Analytical)	Absolute Error
Max Velocity ($\boldsymbol{Umax}$)	0.25219	0.25219	1.2×10^{-5}
$\boldsymbol{Nu}$ at $\boldsymbol{Y = 0}$	5.4133	5.4133	6.3×10^{-5}
$\boldsymbol{Sh}$ at $\boldsymbol{Y = 0}$	1.4133	1.4133	8.9×10^{-5}

Table 4: Transient Velocity at Y=0.5

Time (τ)	Analytical $\boldsymbol{U(0.5, \tau)}$	Numerical $\boldsymbol{U(0.5, \tau)}$
0.10	0.064065	0.064065
0.50	0.320324	0.320324

Steady-State Profiles

Fig. 2a and 2b illustrate velocity profiles for different Gr and Nr respectively. Increasing the Grashof number (Gr) significantly enhances buoyancy, leading to a 637% increase in maximum

velocity as Gr rises from 1 to 10. The velocity peak shifts towards the hotter wall ($Y = 1$). Conversely, increasing the buoyancy ratio (Nr) dampens the flow, reducing the maximum velocity by 23% as Nr increases from 0.5 to 2.0, due to the opposing solutal buoyancy force.

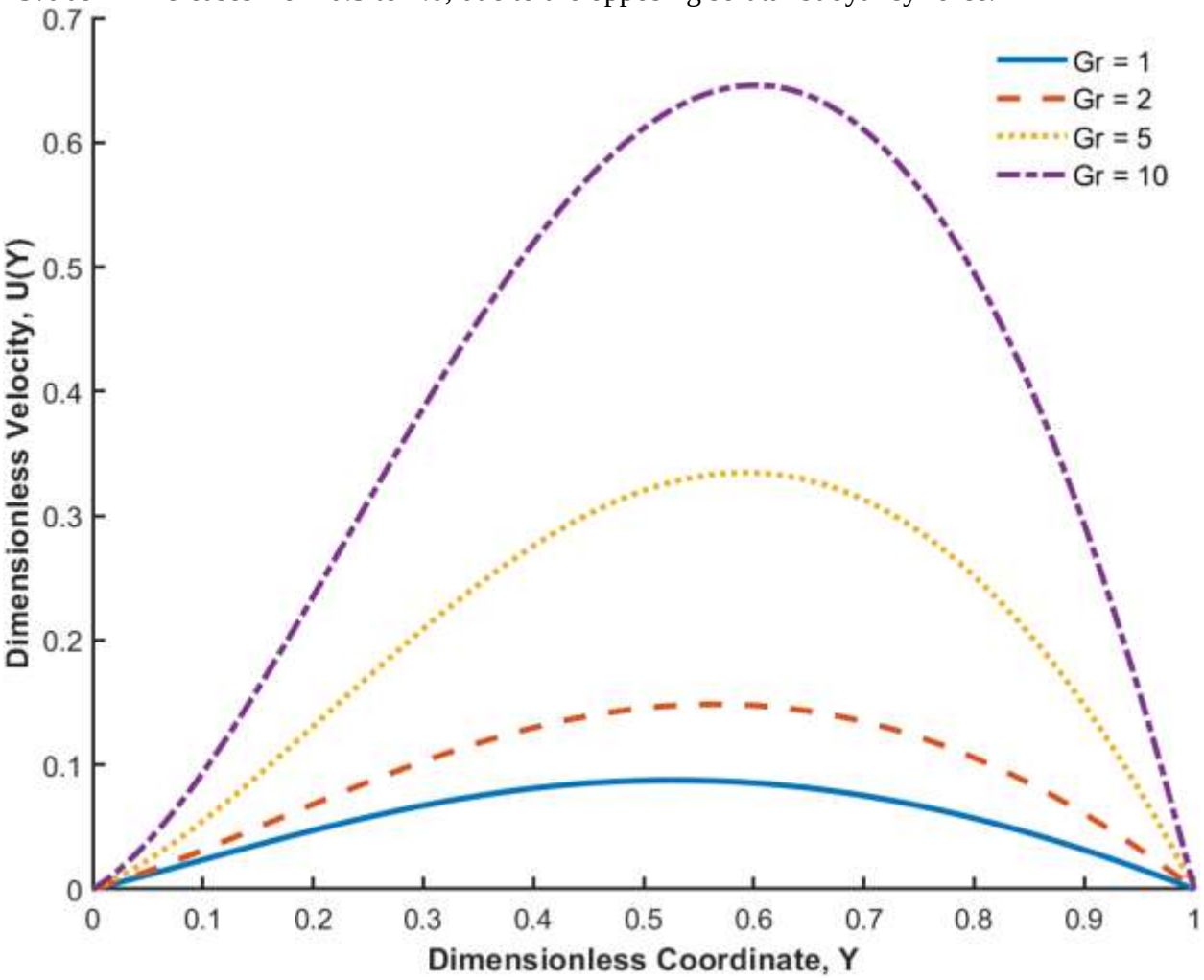

Fig. 2a: Velocity Profiles for Different Grashof Numbers (Gr)

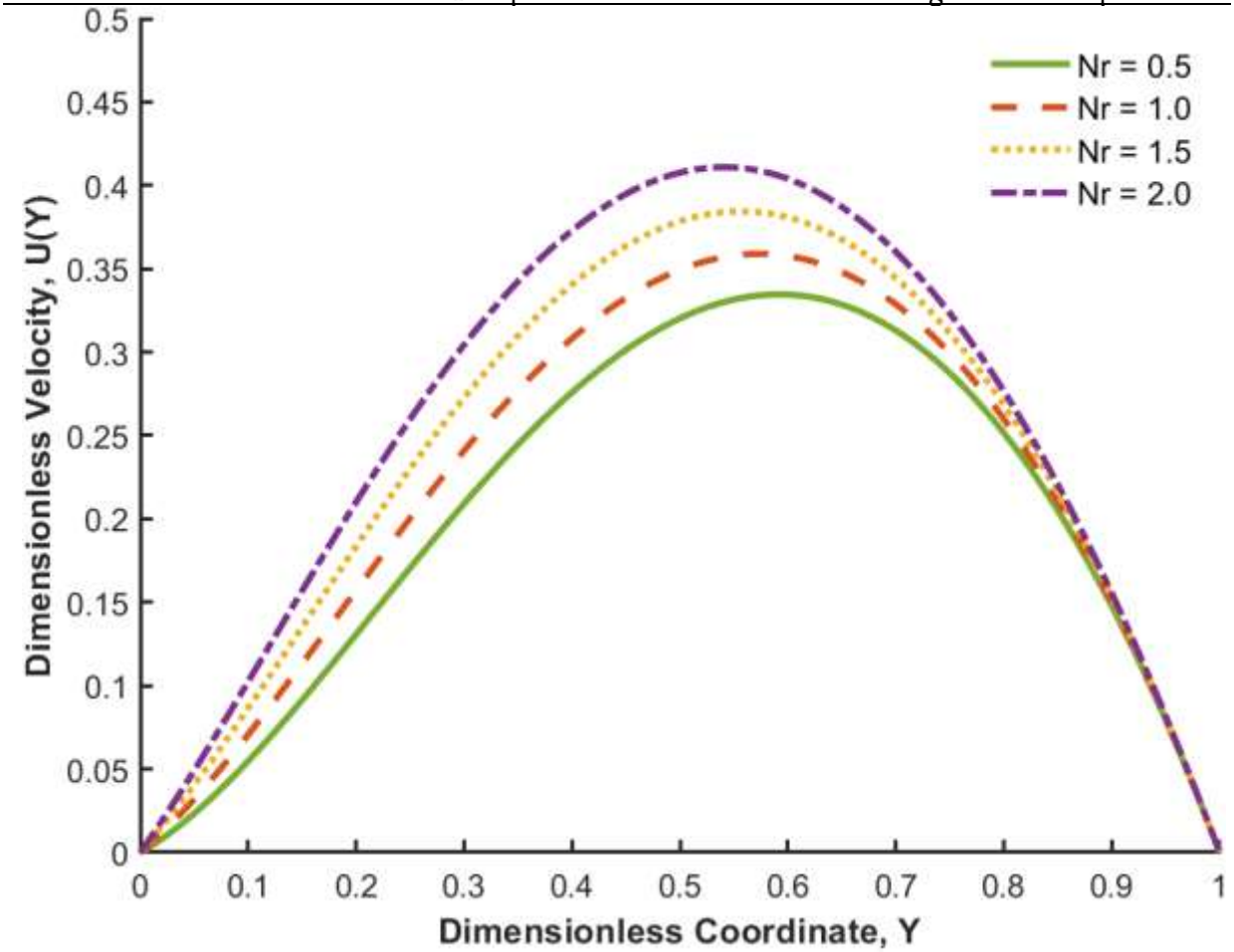

Fig. 2b: Velocity Profiles for Different Buoyancy Ratio Parameter (Nr)

Fig. 3a and 3b show temperature profiles for different Nb and Nt parameters respectively. A higher Brownian motion parameter (Nb) flattens the temperature profile, promoting thermal uniformity via enhanced nanoparticle diffusion. In contrast, a higher thermophoresis parameter (Nt) steepens the temperature gradient near the hot wall, as thermophoresis drives nanoparticles to colder regions, creating a thermal resistance layer.

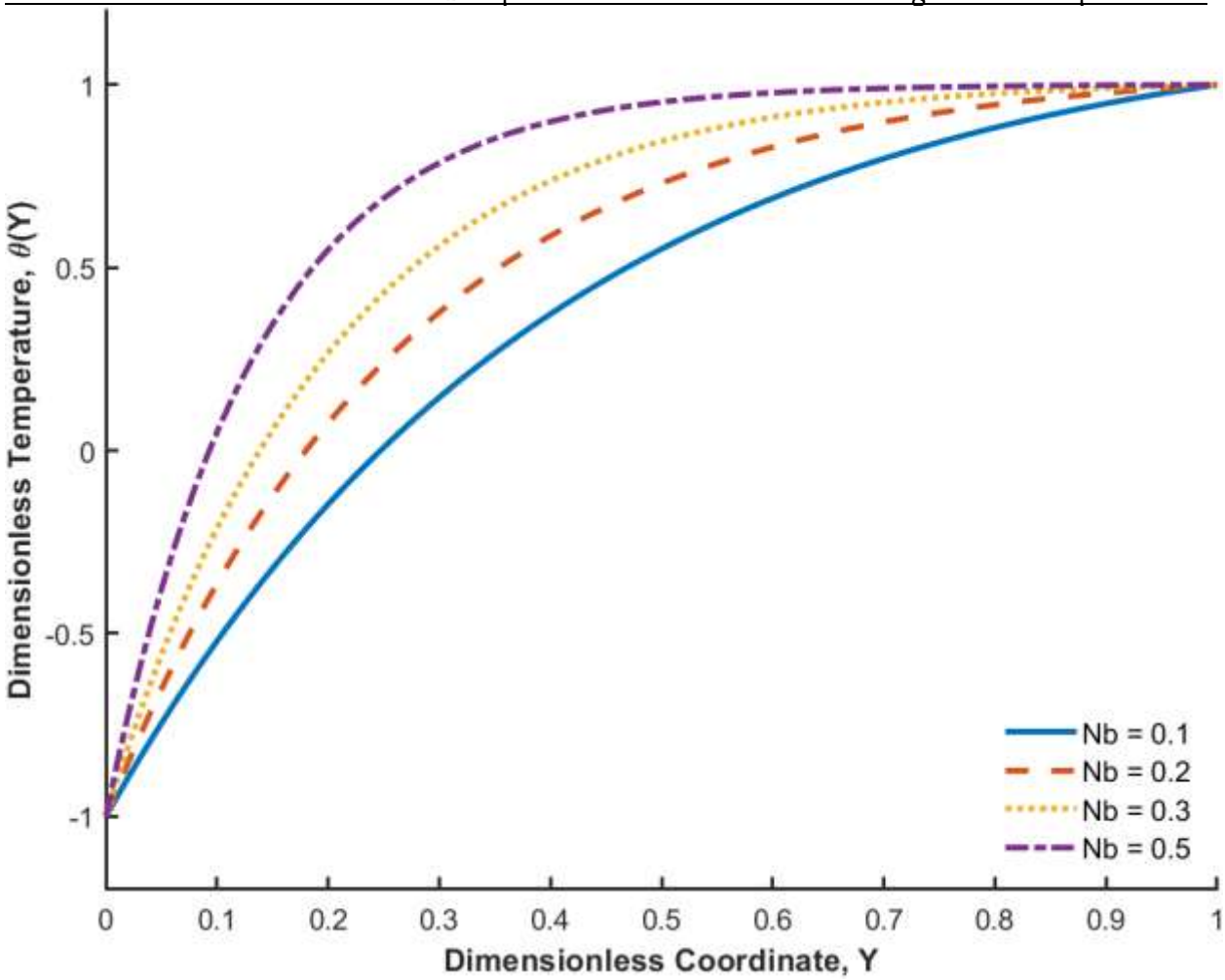

Fig. 3a: Temperature Profiles for Different Brownian Motion (Nb) Parameter

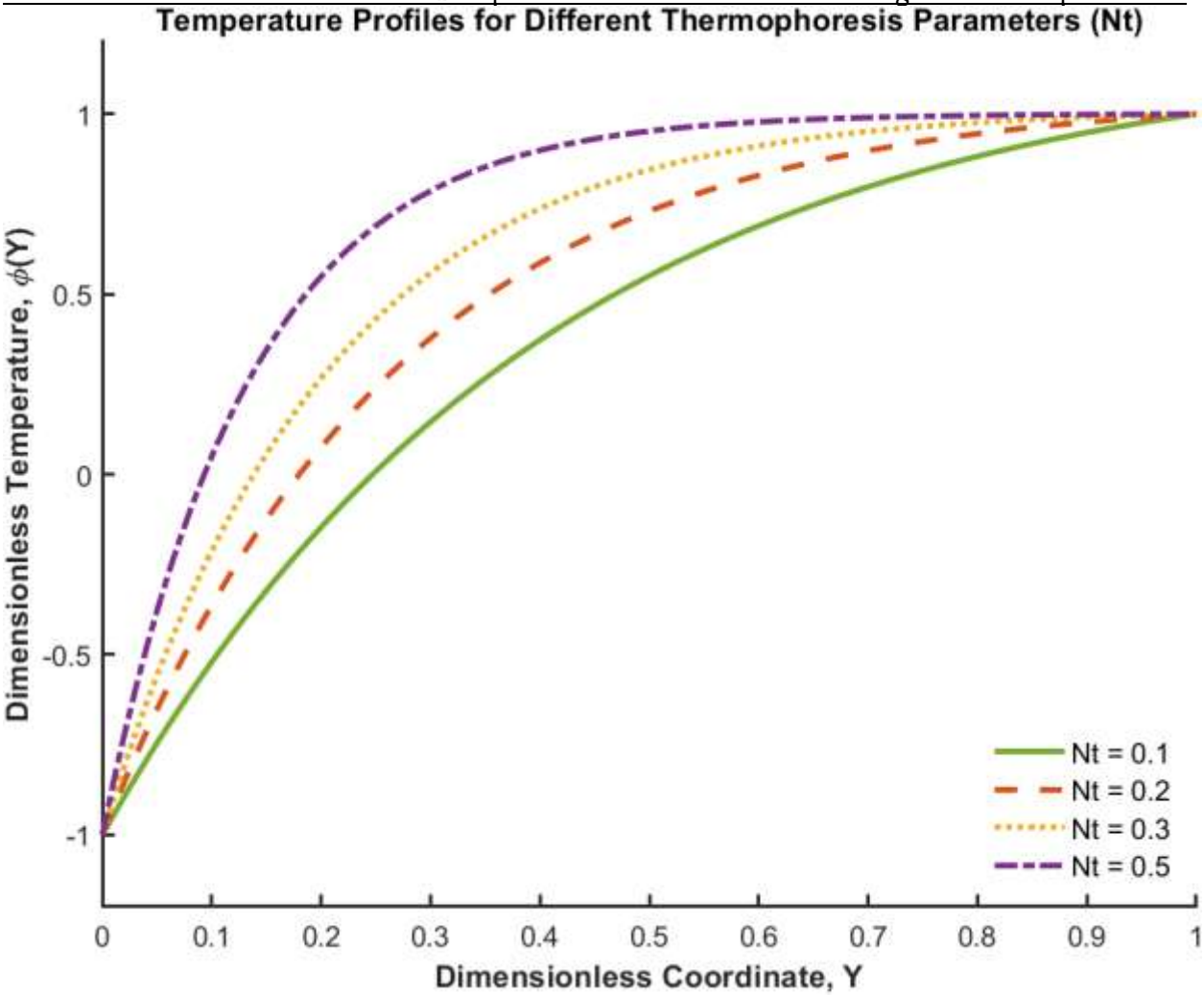

Fig. 3b: Temperature Profiles for Different Thermophoresis (Nt) Parameter

Fig. 4 illustrates concentration profiles with Nt/Nb ratio variations. The ratio Nt/Nb governs the concentration distribution. At low ratios, Brownian diffusion dominates, leading to a nearly linear profile. At high ratios, thermophoresis dominates, causing significant nanoparticle migration towards the cold wall (Y=0), evident as a sharp concentration gradient.

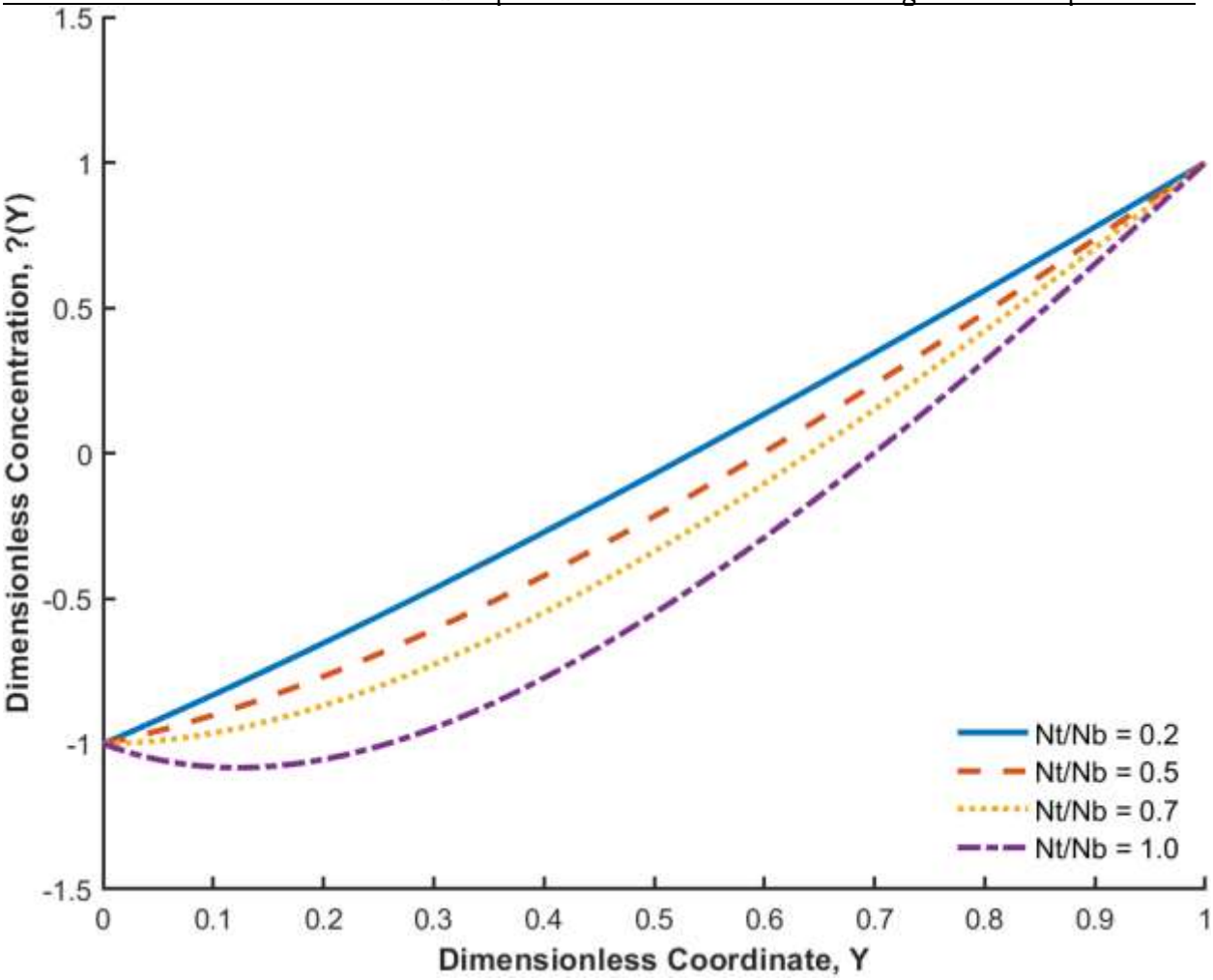

Fig. 4: Concentration Profiles with $\frac{Nt}{Nb}$ ratioVariations

Transient Evolution and Heat/Mass Transfer

The transient evolution from startup to steady-state reveals critical dynamics. Velocity fields develop fastest, reaching steady state around $\tau \approx 3.0$. Thermal fields evolve more slowly ($\tau \approx 2.5$), while nanoparticle concentration, governed by the slower mass diffusion, takes the longest to stabilize ($\tau > 2.0$) as illustrated in Figures 5-7.

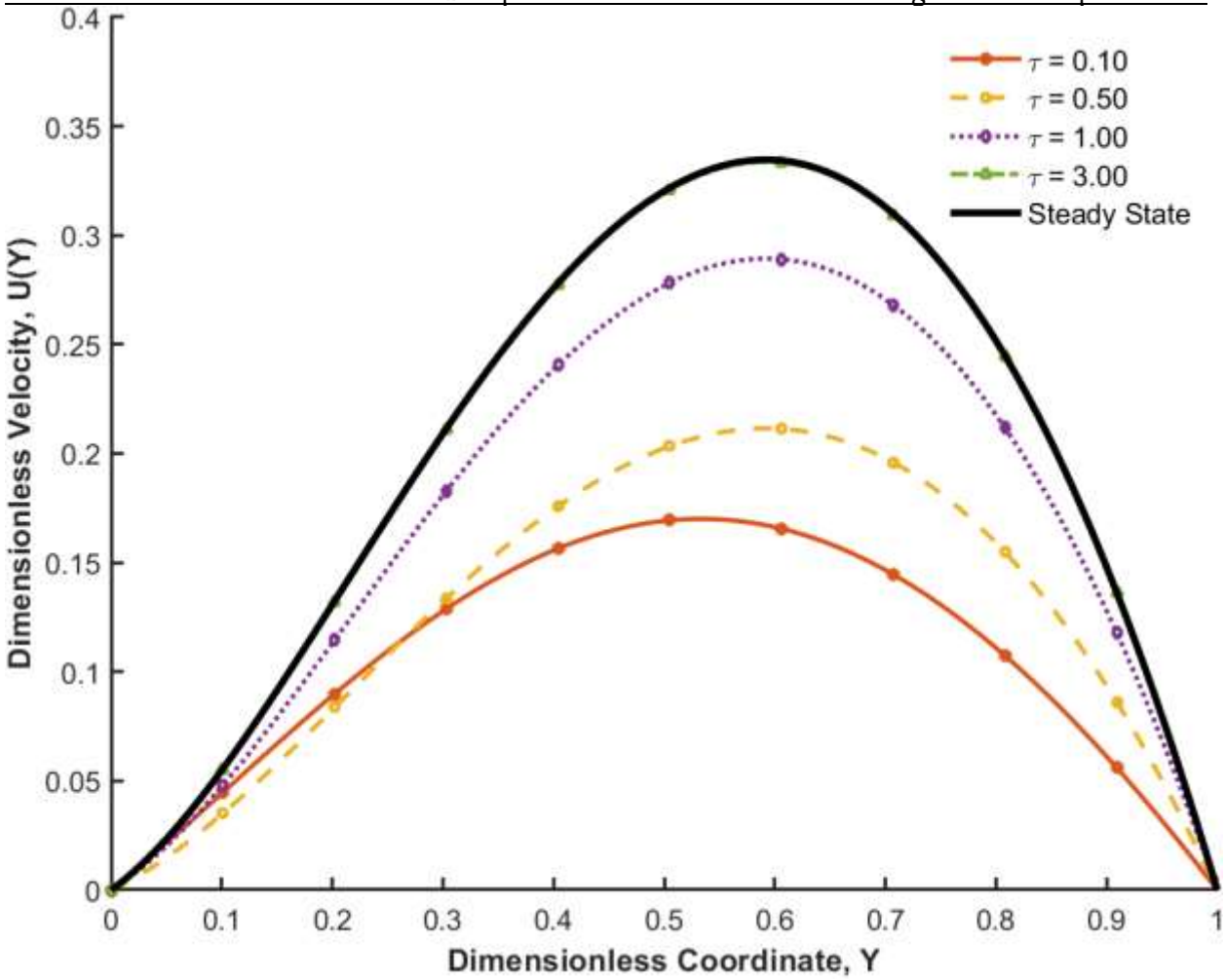

Fig. 5: Velocity Profile Comparison of Steady State and Transient State

European Journal of Mechanical Engineering Research, 12(2),61-78, 2025
Print ISSN: 2055-6551(Print)
Online ISSN: 2055-656X(Online)
Website: https://www.eajournals.org/
Publication of the European Centre for Research Training and Development-UK

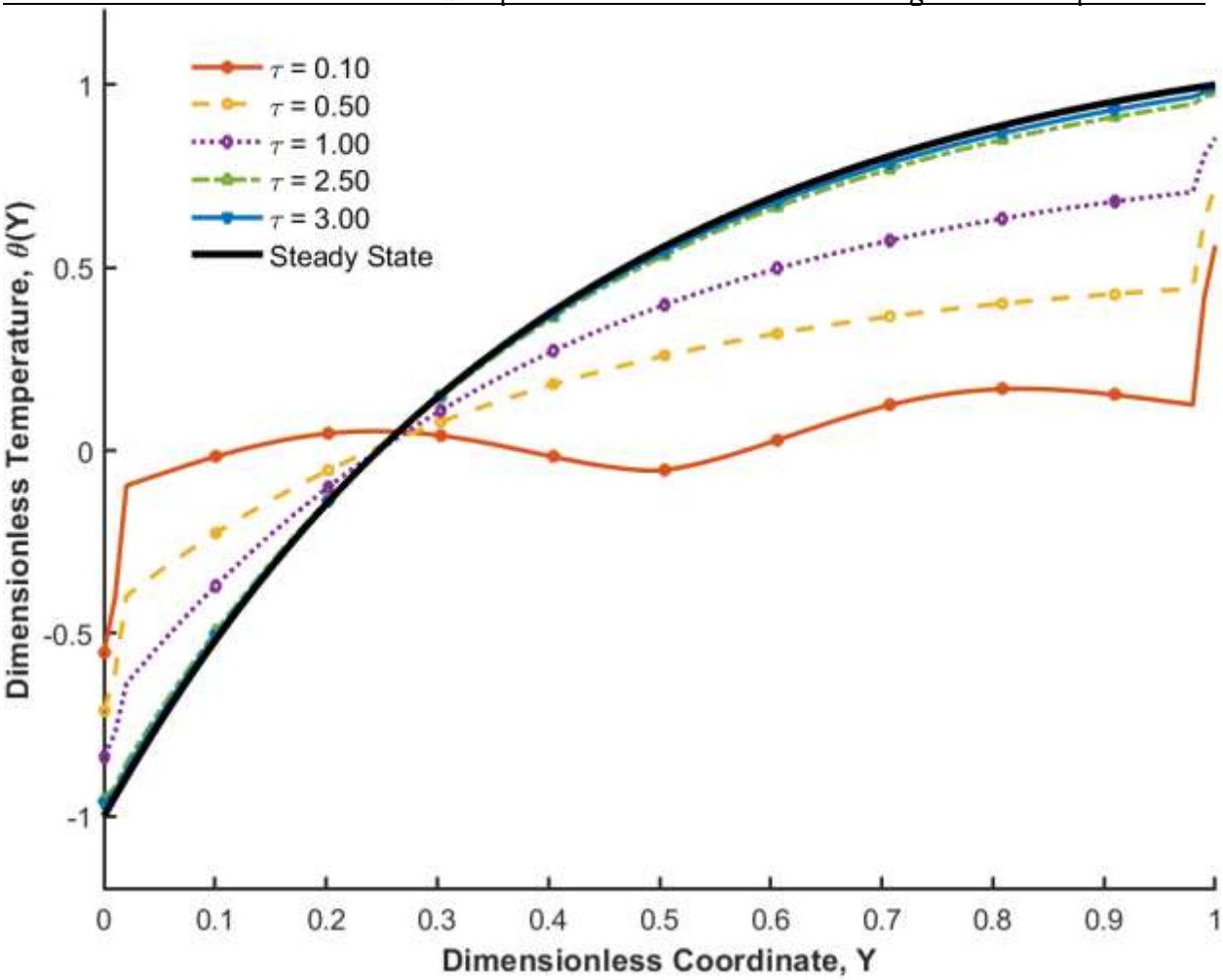

Fig. 6: Temperature Profile Comparison of Steady State and Transient State

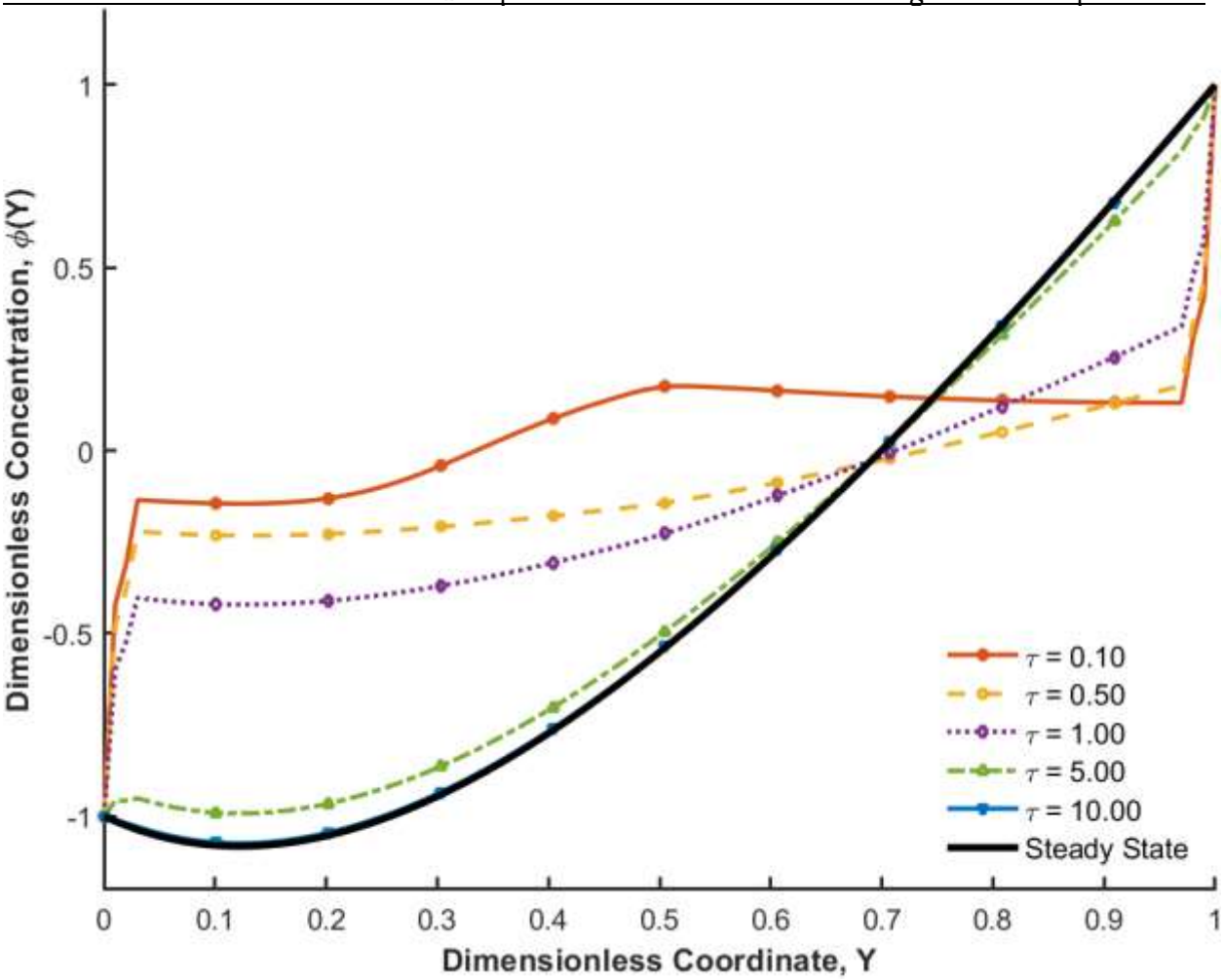

Fig. 7: Concentration Profile Comparison of Steady State and Transient State

Most notably, the Nusselt and Sherwood numbers exhibit significant overshoot during the initial transient phase (Fig. 8 and Fig. 9). The Nusselt number peaks at 39.6% above its steady-state value, and the Sherwood number peaks 28.4% above its steady-state value. This indicates a period of enhanced heat and mass transfer immediately after the initiation of flow, which is crucial for applications involving pulsed or intermittent cooling.

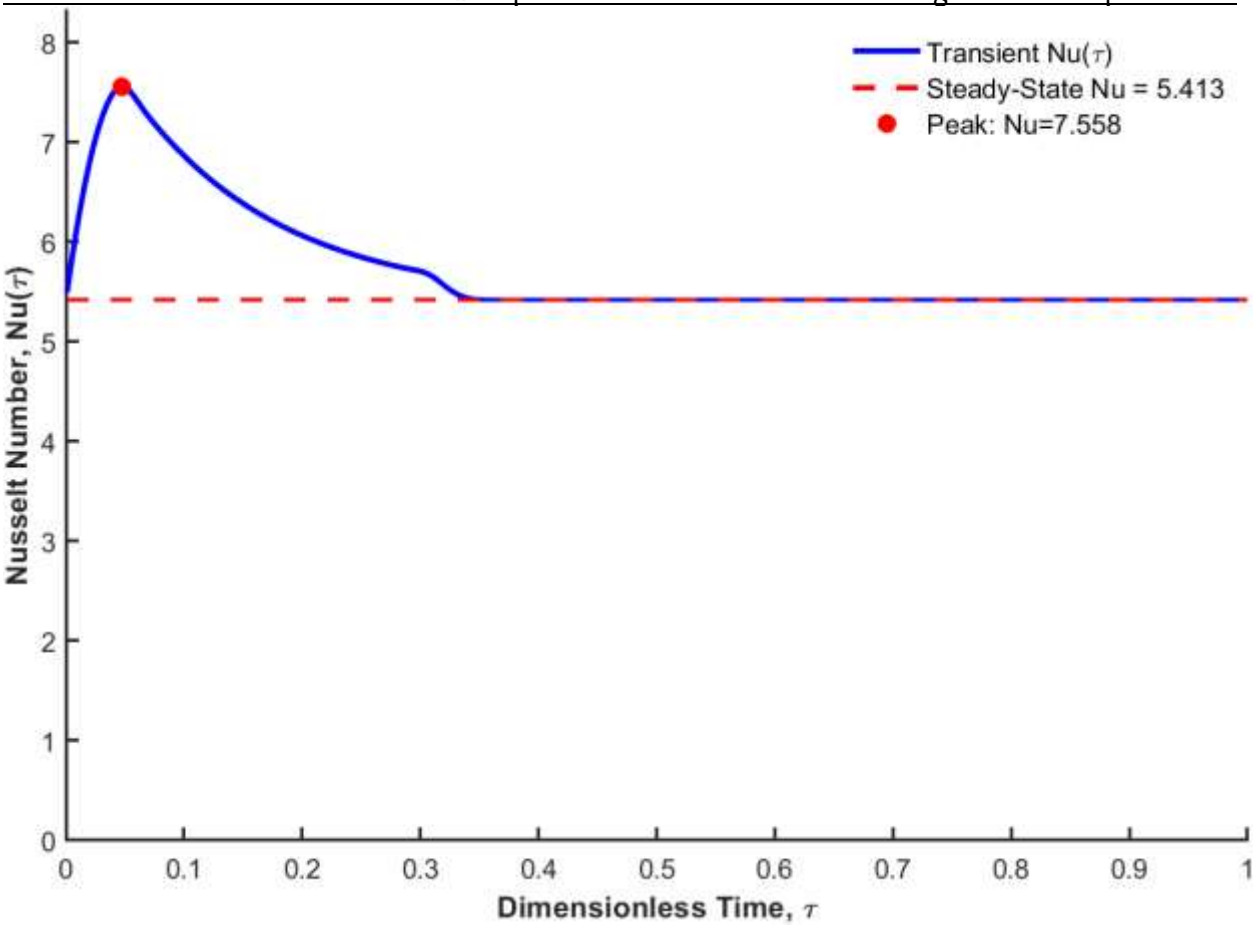

Fig. 8: Nusselt Number Evolution of Transient State and Steady State

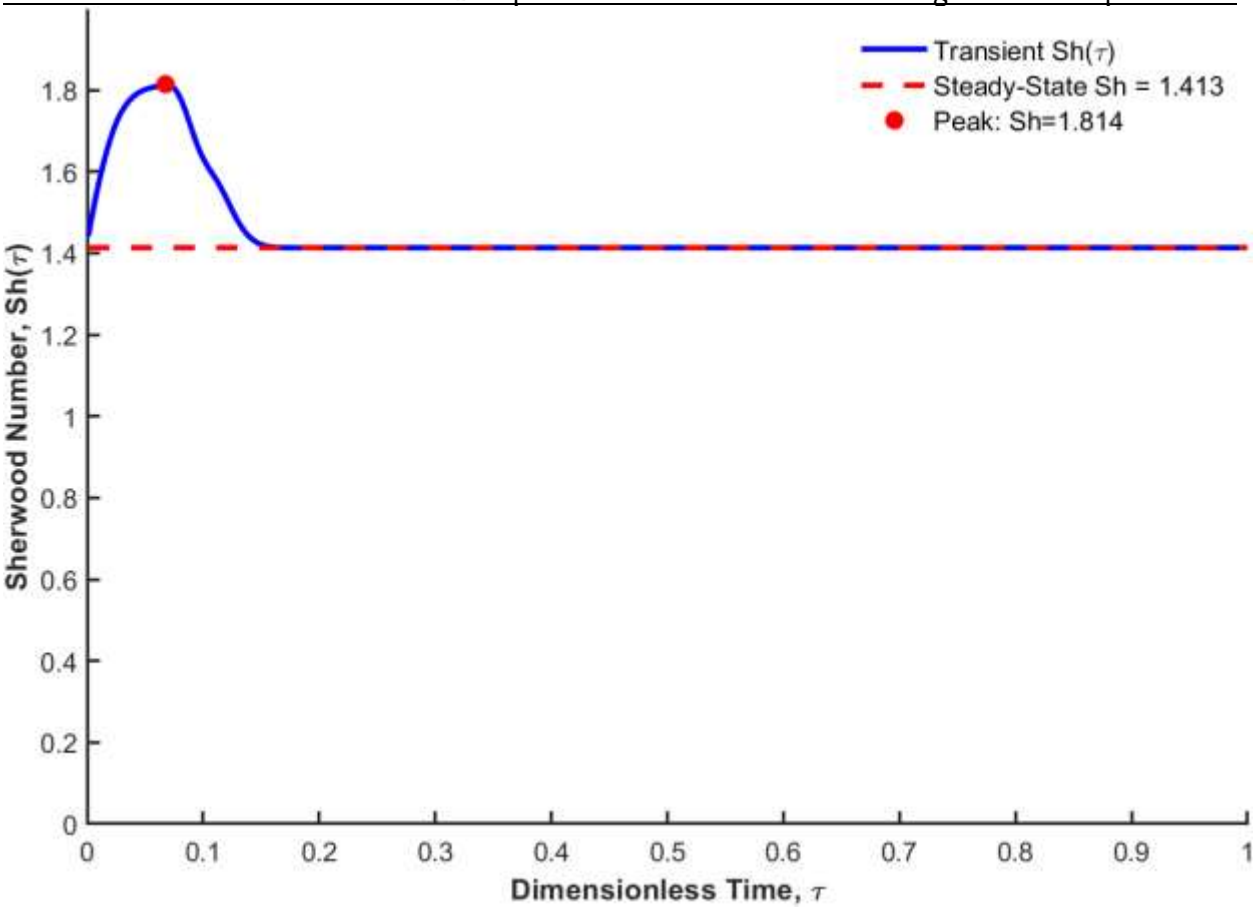

Fig. 9: Sherwood Number Evolution of Transient State and Steady State

CONCLUSION

This study successfully derived exact analytical solutions for steady-state and semi-analytical solutions for transient free convection of nanofluids in a vertical channel. The key findings are:

i. Analytical Solutions: Closed-form solutions for steady-state and semi-analytical solutions for transient state profiles provide a valuable benchmark for validating numerical models in nanofluid research.

ii. Transient Dynamics: The developed Laplace transform solution effectively captures the temporal evolution, revealing significant overshoots in heat and mass transfer rates (Nu and Sh) during early transients, which can be exploited for enhanced thermal performance in dynamic systems.

iii. Parametric Control: The Grashof number (Gr) and buoyancy ratio (Nr) are primary controls for flow intensity, while the Brownian motion (Nb) and thermophoresis (Nt) parameters dictate thermal and concentration distributions. The Nt/Nb ratio is a key design parameter for controlling nanoparticle migration.

iv. Validation: Excellent agreement between analytical, numerical, and benchmark results confirms the accuracy and reliability of the proposed models.

This work provides fundamental insights and practical tools for designing and optimizing nanofluid based thermal systems in electronics cooling, solar energy, and industrial heat exchangers. Future work will focus on experimental validation and extending the model to include magnetic fields, radiative heat transfer, and hybrid nanofluids.

REFERENCES

[1] Tiwari, R. J., Said, Z., Hachicha, A. A., Allouhi, A. & Rahman, S. M. A. (2013). Improved thermal conductivity of nanofluids. *International Journal of Heat and Mass Transfer*, 65, 362–368.

[2] Choi, S. U. S., (1995), "Enhancing Thermal Conductivity of Fluids with Nano particles," *Development and Applications of Non-Newtonian Flows*, D. A. Siginer and H. P. Wang, eds., *ASME*, New York, MD-Vol. 231 and FED-Vol. 66, pp. 99–105.

[3] Buongiorno, J. (2006). Convective Transport in Nanofluids. *ASME J. Heat Transfer*, 128(3), 240-250.

[4] Kuznetsov, A. V. & Nield, D. A. (2010). Natural convective boundary-layer flow of a nanofluid past a vertical plate. *International Journal of Thermal Sciences*, 49(2), 243-247.

[5] Sarki, M. N. & Buhari, A. (2025). Analytical Solution for the Steady State Free Convection Flow of a Nanofluid in a vertical channel. *International Journal of Science for Global Sustainability*, 11(1), DOI: https://doi.org/10.57233/ijsgs.v11i1.783.

[6] Sheikholeslami, M., & Ganji, D. D. (2017). *Numerical Methods for Nanofluid Simulation*. Springer.

[7] Grosan, T. & Pop, I. (2012). Fully developed mixed convection in a vertical channel filled by a nanofluid. *Journal of Heat Transfer*, 134(8), 082501.

[8] Chandran, P., Sacheti, N. C., & Singh, A. K. (2015). Natural convection near a vertical plate with ramped wall temperature. *Heat and Mass Transfer*, 51(6), 831–839. DOI: https://doi.org/10.1007/s00231-014-1456-4